Polymer 83 (2016) 199–204

Contents lists available at ScienceDirect

Polymer

journal homepage: www.elsevier.com/locate/polymer

Fluorinated poly(arylene ether ketone)s for high temperature dielectrics

Andrew T. Shaver [a], Kezhen Yin [b], Hailun Borjigin [a], Wenrui Zhang [a], Shreya Roy Choudhury [a], Eric Baer [b], Sue J. Mecham [a], J.S. Riffle [a, *], James E. McGrath [a]

[a] *Macromolecules and Interfaces Institute, Virginia Tech, Blacksburg, VA, USA*
[b] *Center for Layered Polymeric Systems, Department of Macromolecular Science and Engineering, Case Western Reserve University, Cleveland, OH, USA*

ARTICLE INFO

Article history:
Received 20 August 2015
Received in revised form
20 November 2015
Accepted 3 December 2015
Available online 11 December 2015

Keywords:
Poly(arylene ether ketone)
Capacitor
Dielectric polymer

ABSTRACT

There is a need for polymeric capacitors with improved energy storage density and thermal stability. In this work, the effect of polymer molecular structure and symmetry on T_g, breakdown strength, and relative permittivity were investigated. A systematic series of four amorphous poly(arylene ether ketone)s were compared. Two of the polymers had symmetric bisphenols while the remaining two had asymmetric bisphenols. Two contained trifluoromethyl groups while the other two had methyl groups. The symmetric polymers had T_g's of approximately 160 °C while the asymmetric polymers showed higher T_g's near 180 °C. The symmetric polymers had breakdown strengths near 380 kV/mm at 150 °C. The asymmetric counterparts had breakdown strengths near 520 kV/mm even at 175 °C, with the fluorinated polymers performing slightly better in both cases. The non-fluorinated polymers had higher relative permittivities than the fluorinated materials, with the asymmetric polymers being better in both cases.

1. Introduction

Today's electronics are involved in many vital functions of everyday life and capacitors serve key roles in these devices [1–4]. Because of miniaturization and increased energy consumption in such applications, new dielectric materials must be developed with higher energy density while maintaining low loss of that energy [1,4]. Considerable research has been devoted to polymeric dielectric materials due to their ease of manufacturing, high breakdown strength, low loss, and self-clearing capabilities [1,5,6]. Biaxially oriented polypropylene is widely regarded as the current state-of-the-art material and it is well known that many of its properties originate from the biaxial orientation process [7–10]. However, the use of biaxially oriented polypropylene is limited due to its poor performance above ~85 °C and low energy density [8,9,11].

A processing technique under investigation to increase dielectric film performance has been termed forced assembly microlayer coextrusion [12–20]. In this process, two polymers are multilayered in a film to create a structure with many parallel alternating layers [21]. This is advantageous for capacitors because the properties of two different materials can be combined and each interface of the two polymers works to bolster the overall dielectric properties [12,13]. One of the polymers, the insulating layer with low dielectric constant, is chosen to have high breakdown strength and low loss, e.g. poly(ethylene terephthalate) [19], polycarbonate [12–18], or polysulfone [20]. The other polymer has a high dielectric constant such as poly(vinylidene fluoride) [13,17,20] or it's copolymers that can increase the energy density [12,14–16,18,19]. The layered structure leads to build-up of Maxwell-Wagner-Sillars interfacial polarization at the interfaces. The charge buildup at these interfaces allows the films to discharge along the interfaces and thus results in higher breakdown strengths [19].

In this work, four different poly(arylene ether)s were synthesized to compare symmetric and asymmetric fluorine-containing structures versus their non-fluorinated counterparts. Prior work on low dielectric polymers as insulators showed that asymmetric versus symmetric fluorination could affect a material's overall polarization [22]. Therefore, this paper describes poly(arylene ether ketone)s (PAEKs) with systematic fluorine- and non-fluorine-containing geometries that could be melt processed for use in capacitors (Fig. 1). In the future, they could be layered with poly(vinylidene fluoride) to explore the effect that fluorination and symmetry have on the interfaces of the microlayer film

---

* Corresponding author.
E-mail address: judyriffle@aol.com (J.S. Riffle).

http://dx.doi.org/10.1016/j.polymer.2015.12.006
0032-3861/© 2015 Elsevier Ltd. All rights reserved.

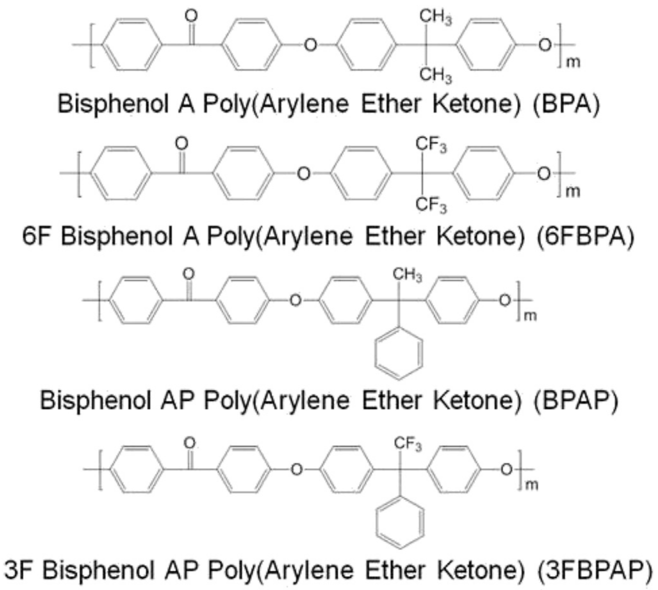

Fig. 1. The polymer chemical structures.

architecture. Literature shows that increasing the strength of the interface can increase the breakdown strength of layered dielectric films [23]. It was reasoned that added fluorine structures in the polymers may improve interactions with fluorinated high dielectric constant materials such as PVDF.

2. Experimental materials

N,N-Dimethylacetamide (DMAc), dichloromethane, triflic acid, toluene, 4,4'-(1-phenylethylidene)bisphenol, 2,2,2-trifluoroaceto phenone, and phenol were purchased from Sigma–Aldrich. DMAc was vacuum distilled from calcium hydride. Triflic acid, toluene, dichloromethane, 2,2,2-trifluoroacetophenone and phenol were used as received. 4,4'-(1-Phenylethylidene)bisphenol was dried at 110 °C under vacuum. 4,4′-Difluorobenzophenone and bisphenol A were kindly donated by Solvay and recrystallized from 2-propanol and toluene, respectively. 4,4′-Hexafluoroisopropylidenediphenol was obtained from Ciba and purified by sublimation, followed by recrystallization from toluene. Potassium carbonate was purchased from Fisher Scientific and dried at 150 °C under vacuum.

2.1. Synthesis of 1,1-bis(4-hydroxyphenyl)-1-phenyl-2,2,2-trifluoroethane (the bisphenol monomer for 3FBPAP)

Phenol (41.32 g, 440 mmol) and 2,2,2-trifluoroacetophenone (19.32 g, 110 mmol) were charged to a 250-mL, three-neck, round bottom flask equipped with a magnetic stir bar, N_2 inlet, and an addition funnel fitted with a drying tube and heated to 45 °C. Once a homogeneous solution was achieved, triflic acid (3.8 mL, 42 mmol) was introduced dropwise while maintaining the temperature at 45 °C. After 1 h, the slurry was treated with 200 mL of hot deionized water and the product was isolated by filtration. The pink solid was stirred in 200 mL of hot deionized water for 30 min, vacuum filtered, and washed with hot water, then dichloromethane. The product was dried at 80 °C under vacuum for 24 h. Yield was ~90%. The mp was 215 °C, consistent with literature [24].

2.2. Synthesis of BPA, 6FBPA, 3FBPAP and BPAP poly(arylene ether ketone)s

The procedure for all four polymers was the same. A representative synthesis of the BPA polymer was adapted from previous literature [25–29]. For example, bisphenol A (67.713 g, 296.6 mmol), 4,4'-difluorobenzophenone (65.643 g, 306.4 mmol), and DMAc (600 mL) were charged to a three-neck flask equipped with a N_2 inlet, mechanical stirrer, and Dean–Stark trap. Toluene (300 mL) and K_2CO_3 (48.352 g, 349.8 mmol) were added to the flask and the Dean–Stark trap was filled with toluene. The apparatus was placed in a silicone oil bath that was heated to 155 °C to begin azeotropic removal of water. After 4 h the toluene and water were removed from the Dean–Stark trap. The oil bath was maintained at 150 °C for 12 h, then the reaction was allowed to cool to room temperature. The polymer solution was filtered to remove any excess K_2CO_3 or by-product salts. The polymer solution was precipitated into deionized water, then the polymer was stirred in deionized water at 80 °C to further assist the removal of salts and solvents. The white polymer was filtered and dried at 110 °C under vacuum. Yield was 81%.

The values for the remaining three reactions were as follows. For the 6FBPA polymer the amounts of the materials were: 4,4′-Hexafluoroisopropylidenediphenol (2.733 g, 8.128 mmol), 4,4'-difluorobenzophenone (1.814 g, 8.468 mmol), DMAc (24 mL), toluene (12 mL), and K_2CO_3 (1.3800 g, 9.985 mmol). Yield was 92%. For the 3FBPAP polymer the amounts of the materials were: 1,1-bis(4-hydroxyphenyl)-1-phenyl-2,2,2-trifluoroethane (9.960 g, 28.93 mmol), 4,4'-difluorobenzophenone (6.481 g, 30.25 mmol), DMAc (24 mL), toluene (12 mL), and K_2CO_3 (6.4370 g, 46.57 mmol). Yield was 82%. For the BPAP polymer the amounts of the materials were: 4,4'-(1-phenylethylidene)bisphenol (2.081 g, 7.167 mmol), 4,4'-difluorobenzophenone (1.600 g, 7.469 mmol), DMAc (24 mL), toluene (12 mL), and K_2CO_3 (1.2300 g, 8.899 mmol). Yield was 89%.

2.3. Proton nuclear magnetic resonance (NMR) spectroscopy

^{1}H NMR analysis was performed on a Varian Inova spectrometer operating at 400 MHz. All spectra were obtained from 15% (w/v) 1-mL solutions in chloroform-d.

2.4. Film-casting

The polymer (0.4 g) was weighed into a small glass vial with a magnetic stir bar. Chloroform (11 mL) was added to the vial to obtain a 2.5 wt% solution. The solution was filtered using a 1-μm syringe filter into a clean glass vial. A 5 × 5″ glass plate was placed in a base bath for 30 min for surface treatment. The glass plate was rinsed and dried, then placed on a level surface for casting. The solution was poured onto the plate and the solution was spread to the edges of the plate until it covered the whole glass plate. A glass dome with 2 outlets was used to cover the plate. One outlet was fitted with a syringe filter and the other was connected to the house air stream running at 2 SCFH. The plate was left undisturbed for a minimum of 30 min, then transferred to an oven at 110 °C for an additional 30 min. The film was removed from the glass plate using a razor blade by slowly lifting the edges until the film came off.

2.5. Size exclusion chromatography (SEC)

SEC was conducted to measure molecular weights and distributions. The mobile phase was DMAc distilled from CaH_2 containing dry LiCl (0.1 M). The column set consisted of 3 Agilent PLgel 10-μm Mixed B-LS columns 300 × 7.5 mm (polystyrene/divinylbenzene) connected in series with a guard column having the same stationary phase. The columns and detectors were maintained at 50 °C. An isocratic pump (Agilent 1260 infinity, Agilent Technologies) with an online degasser (Agilent 1260), autosampler and column oven was used for mobile phase delivery and sample injection. A system of multiple detectors connected in series was used for the analyses. A multi-angle laser light scattering detector (DAWN-HELEOS II, Wyatt Technology Corp.), operating at a wavelength of 658 nm, a viscometer detector (Viscostar, Wyatt Technology Corp.), and a refractive index detector operating at a wavelength of 658 nm (Optilab T-rEX, Wyatt Technology Corp.) provided online results. The system was corrected for interdetector delay and band broadening using a 21,000 g/mole polystyrene standard. Data acquisition and analysis were conducted using Astra 6 software from Wyatt Technology Corp. Validation of the system was performed by monitoring the molar mass of a known molecular weight polystyrene sample by light scattering. The accepted variance of the 21,000 g/mole polystyrene standard was defined as 2 standard deviations (11.5% for M_n and 9% for M_w) derived from a set of 34 runs. Specific refractive index values were calculated based on the assumption of 100% recovery.

2.6. Thermogravimetric analysis (TGA)

Thermal stabilities of the polymers were investigated using a TA Instruments TGA Q5000 under a N_2 atmosphere with the N_2 running at 25 mL/min. The heating rate was 10 °C/min from room temperature to 700 °C.

2.7. Differential scanning calorimetry (DSC)

The thermal properties were investigated with a TA Instruments DSC Q200. The polymers were heated under N_2 to ensure an inert atmosphere at 60 mL/min. The heating rate was 10 °C/min to 350 °C, then the sample was cooled to 0 °C at 10 °C/min. It was heated once more to 350 °C at 10 °C/min and the reported DSC thermograms are from the second scans.

2.8. Refractive indices

The refractive indices of PAEK films were characterized using a 2010 Metricon instrument with a 633 nm laser at room temperature. The PAEK films were brought into contact with the base of a prism with a known refractive index. The laser beam began horizontal (90°) to the prism/polymer interface so all light was totally reflected, and then it rotated until it was normal to the prism/polymer interface (0°). At some angle between 90° and 0° the reflected laser light intensity decreased which indicated the critical angle. The refractive indices of the films were calculated by Snell's Law (equation (1))

$$n_p sin\theta_p = n_f sin\theta_f \tag{1}$$

where n_p and n_f are the refractive indices of the prism and the film, respectively, θ_p is the critical angle and θ_f equaled 90° [30].

2.9. Breakdown strength

Breakdown strengths of the PAEK films were measured with a needle-plane electrode. The needle electrode was the positive side and the diameter of the needle tip was 40 μm. The negative electrode was a 3 × 10 cm rectangular aluminum plate. A Quadtech (Marlborough, MA) Guardian 20-kV HiPot tester was used as the voltage source and the voltage ramp speed was 500 V/s. The breakdown strength measurements were carried out in an oil bath at 25, 75, 125, 150, and 175 °C with twenty repetitions for each film at each temperature.

2.10. Dielectric thermal analysis (DETA)

Dielectric spectroscopy was measured with a frequency sweep from 0.01 Hz to 10000 Hz at 25 °C at a constant voltage of 1 V using a Novocontrol (Hundsangen, Germany) spectrometer. Electrodes on each side of the film were sputtered-coated with gold using an EMS Q300 T sputter coater (Electron Microscopy Science, Quantum Technologies, Ashford, Kent, England). The diameter of the gold electrode was 1 cm. Prior to testing, the films were dried for 24 h at 120 °C. The frequency sweep measurements were carried out at room temperature and the temperature sweep heating rate was 5 °C/min.

3. Results and discussion

The structures, molecular weights and thermal properties of the poly(arylene ether ketone)s were characterized by proton NMR, SEC and DSC. The ^{1}H NMR spectra shown in Fig. 2 confirmed the expected chemical structures. The integral values were consistent with the expected structures and no extraneous peaks were observed.

The SEC results showed that the polymer M_w's were within close range of each other and that high molecular weights had been achieved (Table 1 and Fig. 3). The PDI's were all symmetric and comparable to each other. Step growth polymerization PDI values should ideally be two. The lower values may be due to lower molecular weight chains being lost during precipitation as well as the fact that light scattering calculations of broad molecular weight polymers tend to overestimate the M_n and thereby reduce the PDI.

The DSC thermograms for the four polymers are shown in Fig. 4. The two symmetric polymers have T_g's near 160 °C while the two asymmetric polymers have T_g's near 180 °C. This increase is most likely caused by increased stiffness of the polymer backbone caused by introducing a phenyl substituent into the linking group in the bisphenol monomers. A stiffer backbone requires more energy to begin long-range segmental motion. Both of the fluorine-containing polymers have slightly higher T_g's than their non-fluorinated counterparts. The larger fluorine atom may cause more steric hindrance than the hydrogen, therefore leading to a stiffer polymer structure.

The calculated breakdown strengths of each of the materials as functions of temperature are listed in Table 2. At 25 °C, the trend is 3FBPAP > BPAP > 6FBPA > BPA with a difference of approximately 20 V between each. This can also likely be correlated to stiffness because breakdown strength has been shown to increase with Young's modulus [31,32]. As the temperature is increased, the two asymmetric polymers maintain higher calculated breakdown strengths, most likely due to their higher T_g's and stiffer backbones. Even at 175 °C, the calculated breakdown strengths of the asymmetric polymers are greater than those of the symmetric polymers at 125 °C.

The relative permittivity (ε) was measured from 10^{-1}to10^4 Hz (Fig. 5). The trend in relative permittivity for the four polymers is BPAP > BPA > 3FBPAP > 6FBPA. The differences can be attributed to their fluorine content, introduction of a phenyl ring, and their symmetric versus asymmetric structures. Increased fluorine content in the polymer increases the fractional free volume, and an increase in fractional free volume decreases the amount of polarizable content per unit volume. With less material to be polarized, the relative permittivity will be lower [33]. Thus, it is reasonable to expect that 6FBPA and 3FBPAP would have lower relative permittivities than BPA and BPAP, respectively. Xie et al. made a series of poly(arylene ether ketone)s using 4,4′-difluorobenzophenone

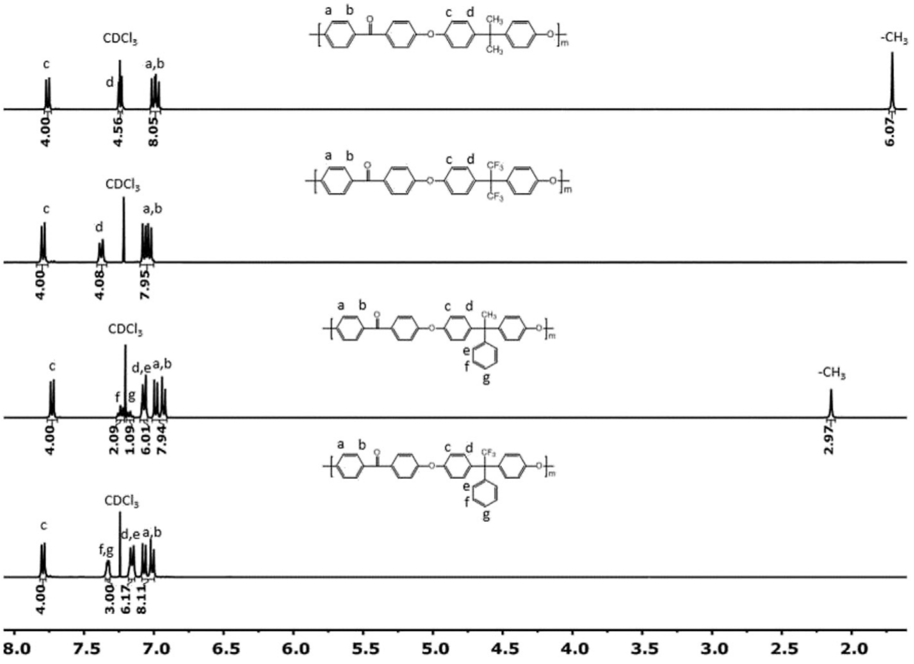

Fig. 2. Confirmation of structure via proton NMR.

Table 1
Molecular weights in DMAc with 0.1 M LiCl at 50 °C

	M_w (kDa)	PDI
BPA PAEK	78	1.5
6FBPA PAEK	67	1.4
BPAP PAEK	67	1.5
3FBPAP PAEK	62	1.4

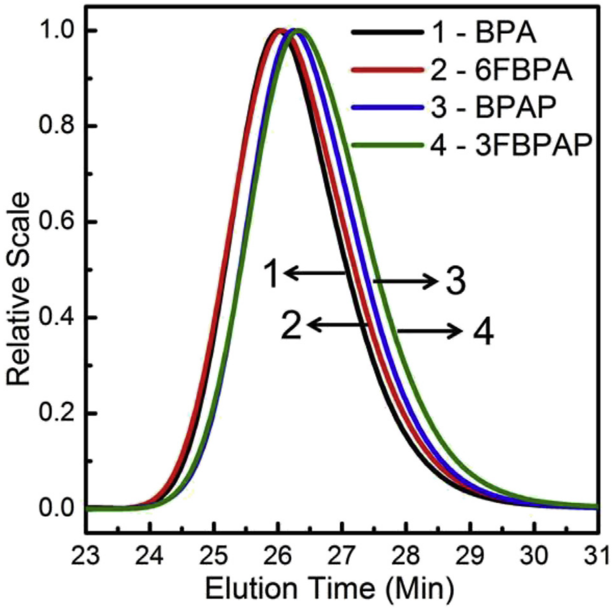

Fig. 3. Molecular weights by light scattering SEC.

which showed comparable results to our own. Their non-fluorinated poly(arylene ether ketone) had an ε of 2.95 at 1 MHz where as our BPA-based poly(arylene ether ketone) had an ε of 2.94 at 0.1 MHz [34]. Further literature shows that the ε of both our fluorinated and non-fluorinated PAEK polymers are in the expected value range. [35–37].

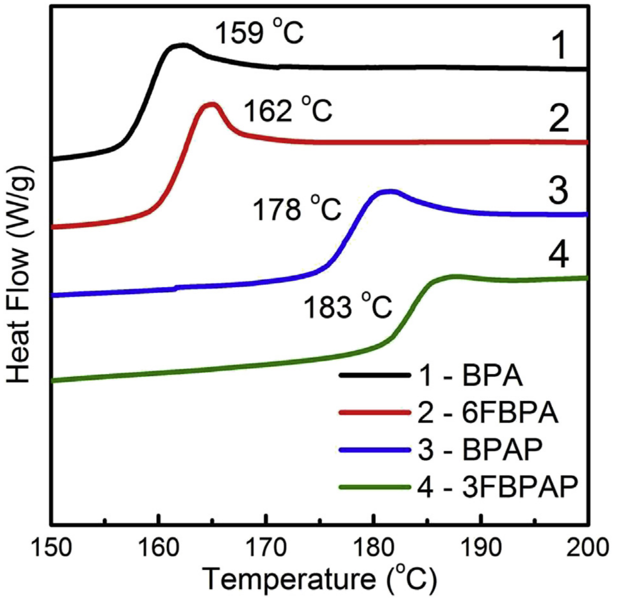

Fig. 4. DSC thermograms showing the glass transition temperatures.

Table 2
Calculated breakdown strengths measured via a needle-plane electrode method. The units of breakdown strength are volts/film thickness (kV/mm).

	25 °C	75 °C	125 °C	150 °C	175 °C
BPA PAEK	782 ± 35	563 ± 44	412 ± 52	365 ± 22	–
6FBPA PAEK	803 ± 55	583 ± 20	410 ± 34	396 ± 28	–
BPAP PAEK	821 ± 45	753 ± 33	651 ± 50	615 ± 27	511 ± 36
3FBPAP PAEK	840 ± 45	765 ± 33	662 ± 49	641 ± 26	523 ± 31

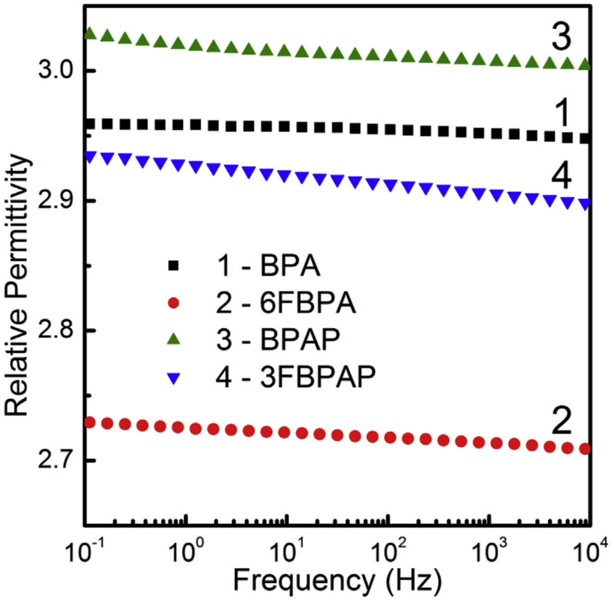

Fig. 5. The relative permittivity of each material over varying frequency at 25 °C.

Introduction of a phenyl ring in the bisphenol linking group increases the relative permittivity because its polarizability to weight contribution is higher than for the methyl or trifluoromethyl groups. This can be explained using the Vogel model polarization group contribution values [38]. The phenyl group has a polarization contribution of 123.5 and a MW of 77 to give a polarizability/weight ratio of 1.604. In comparison, the methyl group has a polarization contribution of 17.66 and a MW of 15 to give a ratio of 1.177. The trifluoromethyl group has a polarization contribution of 86.4 and a MW of 69 to give a ratio of 1.252. The phenyl group contributes more polarization to the relative permittivity than the methyl or trifluoromethyl groups, and this can be correlated to its easily polarized aromaticity [33]. Other poly(ether ketone)s with highly aromatic structures and ketones have high ε values, thus showing their structural importance to the polymer ε for dielectric films [11,39,40].

The higher performance of BPAP and 3FBPAP over their symmetric counterparts, BPA and 6FBPA, can be linked to their asymmetric methyl or trifluoromethyl groups. In the symmetric polymers the methyl or trifluoromethyl groups have an opposing group with the same composition so the dipole will be canceled. Without the opposing group, the asymmetric polymers have a net dipole and any group with a net dipole will contribute to orientation polarization (dipole polarization). Orientation polarization is one of the three main types of polarization that can contribute to the overall polarizability, which is one of the main factors in determining the relative permittivity. The three types are electronic, atomic, and orientation polarization [33].

In order to examine the contribution of incorporating fluorine in an asymmetric geometry, relative permittivities (ε) measured by dielectric spectroscopy were compared with the squares of the refractive indices, also known as the Maxwell ε. Equation (2) shows the relationship between the refractive index and relative permittivity. The difference between the measured and Maxwell ε provides some understanding of the contributions of orientation polarization to the permittivities in the polymer systems. This is because the Maxwell model represents the ε at high frequencies, which is dominated by electronic polarization. The measured ε by dielectric spectroscopy was at lower frequencies and has orientation polarization contributions. Therefore the difference gives an indication of the orientation contribution of the material.

$$\varepsilon_{maxwell} = n^2 \tag{2}$$

In Fig. 6 the left graph compares the measured ε at 1 kHz to the Maxwell ε of the symmetric PAEK structures. The dashed line is included to make a better comparison between the two ε values. The measured ε and Maxwell comparison were extremely close since BPA and 6FBPA are both symmetric and therefore have no orientation polarization. The right graph makes the same comparison but with the two asymmetric structures. In this case there is a difference between the measured ε and the Maxwell comparison lines. This is expected since the orientation polarization due to the asymmetric trifluoromethyl group will be greater than for the asymmetric methyl. This is confirmed since the measured ε by dielectric spectroscopy has a less negative slope than the Maxwell comparison. This indicates that orientation polarization contributes more to the 3FBPAP measured ε than it contributes to the BPAP ε.

4. Conclusions

In summary, we were able to make high molecular weight BPA, 6FBPA, BPAP, and 3FBPAP based poly(arylene ether ketone)s via nucleophilic aromatic substitution step growth polymerization. All four polymers displayed high T_g's with those of the asymmetric PAEK's approximately 20 °C higher than their symmetric counterparts, most likely due to increases in backbone stiffness. Consistent with the DSC results, the breakdown strengths of the asymmetric PAEK's were higher than for the symmetric polymers. The trend in ε was BPAP > BPA > 3FBPAP > 6FBPA and this was attributed to fluorine content, replacement of the methyl or trifluoromethyl in the bisphenol linking groups with the phenyl ring, and the asymmetric structure. Introduction of fluorine in place of hydrogen results in increased fractional free volume, and this reduces the polarizable content per unit volume. The phenyl ring has a superior polarizability to weight ratio. The asymmetric structure results in larger dipoles which contribute to orientation polarization. This was confirmed by comparing the relative permittivities measured at 1 kHz to the Maxwell model relative permittivities (squares of the refractive indices). This suggests that asymmetric structures with higher relative permittivities would be advantageous for multilayer capacitors with PVDF or its copolymers.

It is reasoned that energy storage density would be improved in multilayer films with increased interaction at the interface between the two materials. Thus, our approach has been to design engineering polymers that contain fluorinated groups so that they will interact positively with PVDF at the interfaces between the layers. The maximum energy storage density in an insulating material is proportional to the dielectric constant times the square of the breakdown strength. The breakdown strengths of these amorphous poly(arylene ether ketone)s are higher than the aromatic polycarbonates that were studied previously. For example, at 125 °C, bisphenol A polycarbonate had a calculated breakdown strength of 540 kV/mm[13] while 3FBPAP PAEK has a calculated breakdown strength of 622 kV/mm. Moreover the T_g of bisphenol A polycarbonate is 150 °C whereas the T_g of 3FBPAP PAEK is 183 °C, and both have excellent mechanical properties. Thus, we believe that these poly(arylene ether ketone)s have potential for incorporation into multilayered (thin-film) capacitors with PVDF as a high dielectric constant layer. The processing parameters for making multilayered capacitors through forced assembly microlayer coextrusion and the dielectric properties of those materials with poly(arylene ether ketone)s and high dielectric constant fluorinated

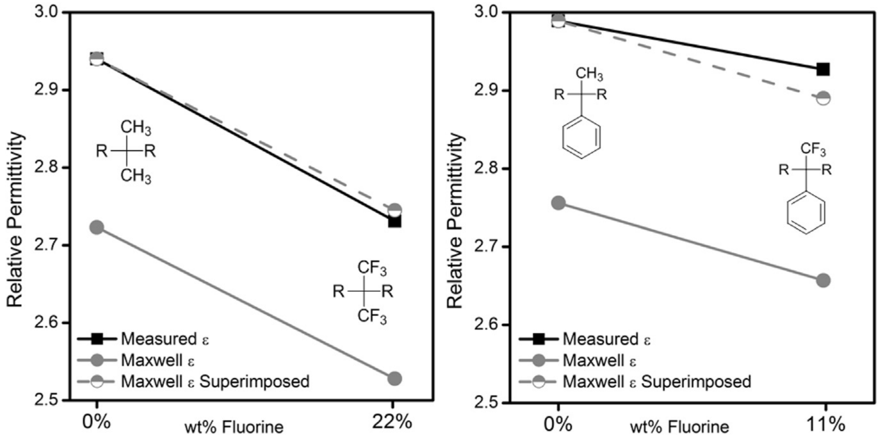

Fig. 6. Comparison of the measured relative permittivity by dielectric spectroscopy versus the squared refractive indices. The left graph is the comparison of the symmetric PAEK structures and the right graph is the comparison of the asymmetric structures. Relative permittivities were measured by dielectric spectroscopy at 1 kHz.

polymers will be a major focus of a forthcoming publication.

Acknowledgments

This research was generously supported by the National Science Foundation through the Center for Layered Polymeric Systems (CLiPS) Science and Technology Center Grant (DMR-0423914).

References

[1] W.J. Sarjeant, J. Zirnheld, F.W. MacDougall, Plasma science, IEEE Trans. 26 (5) (1998) 1368–1392.
[2] L. Zhu, J. Phys. Chem. Lett. 5 (21) (2014) 3677–3687.
[3] F. MacDougall, J. Ennis, Y. Xiao Hui, R.A. Cooper, J.E. Gilbert, J.F. Bates, C. Naruo, M. Schneider, N. Keller, S. Joshi, T.R. Jow, J. Ho, C.J. Scozzie, S.P.S. Yen, High energy density capacitors for pulsed power applications, in: Pulsed Power Conference, 2009. PPC '09. IEEE, June 28, 2009–July 2, 2009, 2009, pp. 774–778.
[4] Z. Shihai, B. Zellers, J. Henrish, S. Rockey, D. Anderson, Z. Chen, Z. Qiming, High energy density film capacitors, in: Pulsed Power Conference, 2009. PPC '09. IEEE, June 28, 2009–July 2, 2009, 2009, pp. 779–783.
[5] W.J. Sarjeant, I.W. Clelland, R.A. Price, Proc. IEEE 89 (6) (2001) 846–855.
[6] N. Venkat, T.D. Dang, Z. Bai, V.K. McNier, J.N. DeCerbo, B.-H. Tsao, J.T. Stricker, Mater. Sci. Eng. B 168 (1–3) (2010) 16–21.
[7] J.L. Nash, Polym. Eng. Sci. 28 (13) (1988) 862–870.
[8] J. Ho, R. Jow, Characterization of High Temperature Polymer Thin Films for Power Conditioning Capacitors, Army Research Lab, Sensors and Electronic Devices Directorate, Adelphi, MD, 2009.
[9] L. Zhu, Q. Wang, Macromolecules 45 (7) (2012) 2937–2954.
[10] E.J. Barshaw, J. White, M.J. Chait, J.B. Cornette, J. Bustamante, F. Folli, D. Biltchick, G. Borelli, G. Picci, M. Rabuffi, Magn. IEEE Trans. 43 (1) (2007) 223–225.
[11] D. Tan, L. Zhang, Q. Chen, P. Irwin, J. Electron. Mater. 43 (12) (2014) 4569–4575.
[12] M.A. Wolak, M.-J. Pan, A. Wan, J.S. Shirk, M. Mackey, A. Hiltner, E. Baer, L. Flandin, Appl. Phys. Lett. 92 (11) (2008) 113301–113303.
[13] M. Mackey, A. Hiltner, E. Baer, L. Flandin, M.A. Wolak, J.S. Shirk, J. Phys. D Appl. Phys. 42 (17) (2009) 175304 (12 pp).
[14] Z. Zhou, M. Mackey, J. Carr, L. Zhu, L. Flandin, E. Baer, J. Polym. Sci. Part B Polym. Phys. 50 (14) (2012) 993–1003.
[15] Z. Zhou, J. Carr, M. Mackey, K. Yin, D. Schuele, L. Zhu, E. Baer, J. Polym. Sci. Part B Polym. Phys. 51 (12) (2013) 978–991.
[16] M. Mackey, D.E. Schuele, L. Zhu, E. Baer, J. Appl. Phys. 111 (11) (2012) 113702–113702-9.
[17] M. Mackey, D.E. Schuele, L. Zhu, L. Flandin, M.A. Wolak, J.S. Shirk, A. Hiltner, E. Baer, Macromolecules 45 (4) (2012) 1954–1962.
[18] M.A. Wolak, A.S. Wan, J.S. Shirk, M. Mackey, A. Hiltner, E. Baer, J. Appl. Polym. Sci. 123 (4) (2012) 2548–2557.
[19] J.M. Carr, M. Mackey, L. Flandin, D. Schuele, L. Zhu, E. Baer, J. Polym. Sci. Part B Polym. Phys. 51 (11) (2013) 882–896.
[20] J.-K. Tseng, C. Lewis, M. Mackey, J. Carr, E. Baer, L. Zhu, PMSE Prepr. (2012).
[21] M. Ponting, A. Hiltner, E. Baer, Macromol. Symp. 294 (1) (2010) 19–32.
[22] G. Hougham, G. Tesoro, A. Viehbeck, J.D. Chapple-Sokol, Macromolecules 27 (21) (1994) 5964–5971.
[23] R. Vogelsang, T. Farr, K. Frohlich, Dielectrics and electrical insulation, IEEE Trans. 13 (2) (2006) 373–382.
[24] S.-H. Hsiao, H.-W. Chiang, Eur. Polym. J. 40 (8) (2004) 1691–1697.
[25] S.A. Srinivasan, J.E. McGrath, High. Perform. Polym. 5 (4) (1993) 259–274.
[26] T.P. Bender, R.A. Burt, G.K. Hamer, C. DeVisser, P.F. Smith, M. Saban, Org. Process Res. Dev. 6 (5) (2002) 714–720.
[27] G.D. Lyle, J.S. Senger, D.H. Chen, S. Kilic, S.D. Wu, D.K. Mohanty, J.E. McGrath, Polymer 30 (6) (1989) 978–985.
[28] Y. Chen, R. Guo, C.H. Lee, M. Lee, J.E. McGrath, Int. J. Hydrogen Energy 37 (7) (2012) 6132–6139.
[29] G.D. Lyle, H. Grubbs, C. Tchatchoua, J.E. McGrath, Polym. Mater. Sci. Eng. 69 (1993) 238–239.
[30] Metricon Oper. Manual.
[31] L.A. Dissado, J.C. Fothergill, Electrical degradation and breakdown in polymers, P. Peregrinus (1992).
[32] H.K. Kim, F.G. Shi, Dielectrics and Electrical Insulation, IEEE Trans 8 (2) (2001) 248–252.
[33] A. Zulkifli, Polymer dielectric materials, in: M.A. Silaghi (Ed.), Dielectric Materials, Intech, Rijeka, Croatia, 2012, pp. 3–26.
[34] J. Xie, W.-Y. Peng, G. Li, J.-M. Jiang, JFBI 3 (3) (2010) 142–147.
[35] H. Treichel, G. Ruhl, P. Ansmann, R. Würl, C. Müller, M. Dietlmeier, Microelectron. Eng. 40 (1) (1998) 1–19.
[36] F. Mercer, T. Goodman, J. Wojtowicz, D. Duff, J. Polym. Sci. Part A Polym. Chem. 30 (8) (1992) 1767–1770.
[37] W.M. Frank, W.D. David, D.G. Timothy, B.W. Janusz, Fluorinated poly(arylene ethers) with low dielectric constants, in: Polymers for Microelectronics, vol. 537, American Chemical Society, 1993, pp. 526–534.
[38] D.W. van Krevelen, K. te Nijenhuis, Properties of Polymers: Their Correlation with Chemical Structure; Their Numerical Estimation and Prediction from Additive Group Contributions, fourth ed., Elsevier Science, 2009.
[39] J. Pan, K. Li, J. Li, T. Hsu, Q. Wang, Appl. Phys. Lett. 95 (2) (2009) 022902–022903.
[40] J. Pan, K. Li, S. Chuayprakong, T. Hsu, Q. Wang, ACS Appl. Mater. Interfaces 2 (5) (2010) 1286–1289.